

The triton in a finite volume

Simon Kreuzer and H.-W. Hammer

*Helmholtz-Institut für Strahlen- und Kernphysik (Theorie)
and Bethe Center for Theoretical Physics,
Universität Bonn, 53115 Bonn, Germany*

(Dated: May 28, 2018)

Abstract

Understanding the volume dependence of the triton binding energy is an important step towards lattice simulations of light nuclei. We calculate the triton binding energy in a finite cubic box with periodic boundary conditions to leading order in the pionless effective field theory. Higher order corrections are estimated and the proper renormalization of our results is verified explicitly. We present results for the physical triton as well as for the pion-mass dependence of the triton spectrum near the “critical” pion mass, $M_\pi^{crit} \approx 197$ MeV, where chiral effective field theory suggests that the nucleon-nucleon scattering lengths in the 1S_0 - and 3S_1 -channels diverge simultaneously. An extension of the Lüscher formula to the three-body system is implicit in our results.

arXiv:1008.4499v1 [hep-lat] 26 Aug 2010

Although Quantum Chromodynamics (QCD) is widely accepted as the underlying theory of strong interactions, ab initio calculations of nuclear properties in Lattice QCD remain one of the largest theoretical challenges in the Standard Model [1, 2]. In nuclear physics, the relevant degrees of freedom are pions and nucleons. Traditionally, their interactions are described via phenomenological potentials fitted to the nucleon-nucleon scattering data. More recently, the advent of model independent Effective Field Theory (EFT) approaches has allowed for accurate calculations of low-energy nuclear physics observables with a direct connection to QCD via its symmetries [3–6].

In Lattice QCD, the QCD path integral is evaluated in a discretized Euclidean space-time using Monte Carlo simulations [7]. However, this approach requires a large numerical effort that strongly constrains the parameters of the simulation. In particular, one is at present forced to use relatively small finite volumes. The energy of states calculated in the finite volume is shifted relative to the infinite volume limit [8]. This shift has to be taken into account when extracting physical observables from lattice simulations. The finite volume also allows for the extraction of scattering observables away from kinematic thresholds. By generalizing a quantum mechanical result to field theory, Lüscher showed that the volume dependence of two-body energy states encodes the infinite volume scattering phase shift [9] as well as resonance properties [10]. An extension of these results to the three-body sector is required for the simulation of light nuclei and their scattering properties in Lattice QCD.

This necessity motivates our investigation of the volume dependence of the triton binding energy within the pionless EFT. This EFT is valid for processes with typical momenta below the pion mass and has successfully been applied to describe the properties of light nuclei [3, 4, 6]. To leading order, the triton properties are determined by the nucleon-nucleon scattering lengths in the 1S_0 and 3S_1 channels and a Wigner SU(4) symmetric three-body force [11]. The triton has been considered in pionless EFT in a nuclear lattice formalism but the volume dependence was not investigated [12]. Higher-order corrections to the amplitude including the ones due to 2N effective range terms can be treated perturbatively [13]. The inclusion of such corrections in the pionless EFT has been studied extensively [14–17]. Our strategy to calculate the modification of the triton in a cubic box has previously been employed to investigate bound states of three bosons with large scattering length [18, 19]. In a different approach, Epelbaum and collaborators have calculated the energy of the triton in a finite volume by implementing a discretized version of chiral EFT on a lattice [20]. The correlation function for the three-nucleon system in the triton channel has also been calculated in Lattice QCD recently [21], but because of the relatively large uncertainties no triton properties could be extracted.

Another motivation for our work is the observation that QCD lies close to an infrared renormalization group limit cycle [22]. The pion mass dependence of the nucleon-nucleon scattering lengths from chiral EFT is compatible with simultaneously diverging nucleon-nucleon scattering lengths in the 1S_0 as well as in the 3S_1 channel near a critical pion mass $M_\pi^{crit} \approx 197$ MeV [23–25]. As a consequence, it was conjectured that QCD could be tuned to the limit cycle by slightly changing the up and down quark masses [22]. In this scenario, excited states of the triton would appear near the critical quark masses. At the critical point itself, the triton would have infinitely many excited states with an accumulation point at threshold. This is a signature of the universal Efimov effect which appears in three-body systems with resonant short-range interactions [26]. It has recently been observed experimentally in atomic systems [27] and many nuclear systems can be described in an expansion around the ideal Efimov limit [28, 29]. The large scattering lengths make the

region near the critical pion mass accessible to the pionless EFT, whose input parameters for various pion masses can be obtained from chiral EFT. This program has successfully been carried out to next-to-next-to-leading order (N²LO) in the infinite volume [30, 31]. When investigating this pion mass region with Lattice QCD, it is again desirable to have control over the effects of the finite volume. In particular, the influence of the finite volume on the infrared limit cycle is not known.

To leading order in the pionless EFT, the Lagrangian for a system of three nucleons can be written as [11]

$$\begin{aligned} \mathcal{L} = & N^\dagger \left(i\partial_t + \frac{1}{2}\nabla^2 \right) N + \frac{g_t}{2} t_j^\dagger t_j + \frac{g_s}{2} s_A^\dagger s_A \\ & - \frac{g_t}{2} [t_j^\dagger (N^T \tau_2 \sigma_j \sigma_2 N) + \text{h.c.}] - \frac{g_s}{2} [s_A^\dagger (N^T \sigma_2 \tau_A \tau_2 N) + \text{h.c.}] + \mathcal{L}_3, \end{aligned} \quad (1)$$

where the units have been set such that $\hbar = m = 1$ and σ_j (τ_A) are the Pauli matrices acting in spin (isospin) space. The degrees of freedom in this Lagrangian are the nucleon field N and two auxiliary dinucleon fields, t_j and s_A . The field t_j (s_A) corresponds to two nucleons in the 3S_1 (1S_0)-channel. The SU(4)-invariant three-body interaction contained in \mathcal{L}_3 is proportional to $(N^\dagger N)^3$. It can be written as a dinucleon-nucleon contact interaction with a dimensionless coupling constant $H(\Lambda)$ [11],

$$\begin{aligned} \mathcal{L}_3 = & - \frac{2H(\Lambda)}{\Lambda^2} \left(g_t^2 N^\dagger (t_j \sigma_j)^\dagger (t_i \sigma_i) N + \frac{g_t g_s}{3} [N^\dagger (t_j \sigma_j)^\dagger (s_A \tau_A) N + \text{h.c.}] \right. \\ & \left. + g_s^2 N^\dagger (s_A \tau_A)^\dagger (s_B \tau_B) N \right), \end{aligned} \quad (2)$$

where Λ is the momentum cutoff. Finite-range corrections can be incorporated as higher orders in the EFT [14–17] but will not be considered here. The coupling constants $g_{s,t}$ can be matched to the two-body scattering lengths $a_{s,t}$ in the corresponding channel or, in the case of g_t , to the deuteron binding energy. The three-body coupling $H(\Lambda)$ approaches an ultraviolet limit cycle for large Λ . The analytic dependence of H on the cutoff can be expressed as

$$H(\Lambda) = \frac{\cos [s_0 \log(\Lambda/\Lambda_*) + \arctan s_0]}{\cos [s_0 \log(\Lambda/\Lambda_*) - \arctan s_0]}, \quad (3)$$

where $s_0 = 1.00624\dots$ and the phase Λ_* has to be fixed from a three-body datum. The low-energy constant Λ_* is also known as the “three-body parameter”. This renormalization procedure remedies the incorrect ultraviolet behavior of the EFT. Once Λ_* has been fixed from a three-body datum, all other low-energy three-body observables can be predicted. For more details on the infinite volume case we refer the reader to the literature [11, 14–17].

We now consider placing the system inside a cubic box. The finite volume modifies the infrared regime due to momentum quantization. In a finite cubic volume with edge length L and periodic boundary conditions, the allowed momenta are given by $\frac{2\pi}{L}\vec{n}$, $\vec{n} \in \mathbb{Z}^3$, yielding a low-momentum scale $\frac{2\pi}{L}$ corresponding to the minimal accessible non-zero momentum. As long as this scale is small compared to the high-energy scale given by the momentum cutoff Λ , the ultraviolet behavior of the amplitudes is unaffected by the finite volume and the renormalized values for the coupling constants obtained in the infinite volume can be used for finite volume calculations. We will explicitly verify that this claim holds for our results.

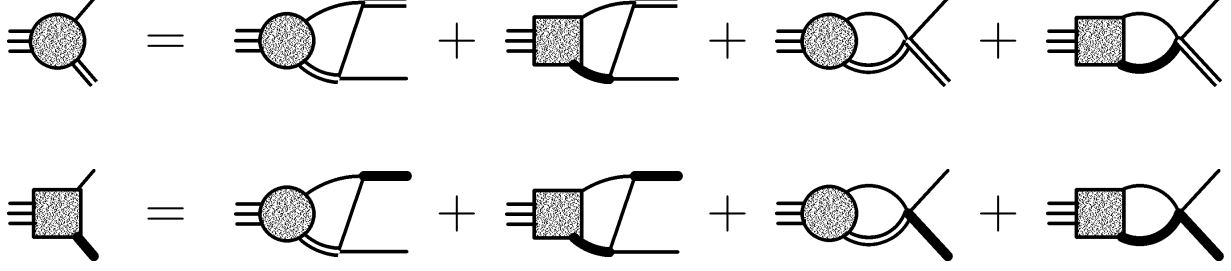


FIG. 1: Integral equation for the triton amplitudes \mathcal{F}_t (shaded circle) and \mathcal{F}_s (shaded square). Single lines denote nucleons, double lines indicate dinucleons in the 3S_1 channel and thick solid lines denote dinucleons in the 1S_0 channel.

The properties of the triton are determined by the bound state amplitude in the spin-1/2 channel which is given by the integral equation in Fig. 1. This equation has non-trivial solutions only for negative energies E_3 whose absolute values correspond to the binding energies. The triton amplitude has two components \mathcal{F}_t (shaded circle) and \mathcal{F}_s (shaded square) that correspond to the outgoing dinucleon being in the 3S_1 and 1S_0 channels. The single lines denote nucleons, while the double and thick solid lines indicate full dinucleon propagators in the 3S_1 and 1S_0 channels, respectively. The amplitude gets contributions from one-nucleon exchange as well as from the three-body interaction in \mathcal{L}_3 . The loop momenta in this equation are quantized in a finite volume as described above. The full propagator for the dinucleon fields is obtained by dressing the bare propagator from Eq. (1) with nucleon loops to all orders. This yields an geometric series of diagrams that can be evaluated analytically:

$$D_{s,t}(p_0, \vec{p}) = \frac{8\pi}{g_{s,t}^2} \left[-\frac{1}{a_{s,t}} + \sqrt{-p_0 + \vec{p}^2/4 - i\epsilon} - \sum_{\substack{\vec{j} \in \mathbb{Z}^3 \\ \vec{j} \neq \vec{0}}} \frac{1}{|\vec{j}|L} e^{-|\vec{j}|L\sqrt{-p_0 + \vec{p}^2/4 - i\epsilon}} \right]^{-1}. \quad (4)$$

The result reproduces the infinite volume dinucleon propagator except for a volume dependent term that vanishes in the limit $L \rightarrow \infty$.

Using the Feynman rules from the Lagrangian in Eqs. (1) and (2) and the full dimer propagators from above, we can explicitly write down the coupled integral equations for the triton amplitude from Fig. 1. It involves integrations over the loop energy and sums over the quantized loop momenta. The integrations are performed by virtue of the residue theorem while the sums over the quantized momenta are rewritten into sums of integrals using Poisson's resummation formula $\sum_{\vec{m} \in \mathbb{Z}^3} \delta^{(3)}(\vec{x} - \vec{m}) = \sum_{\vec{n} \in \mathbb{Z}^3} e^{2\pi i \vec{x} \cdot \vec{n}}$, which is understood to be used under an integral. After projection on the quantum numbers of the triton, we have

$$\begin{pmatrix} \mathcal{F}_t(\vec{p}) \\ \mathcal{F}_s(\vec{p}) \end{pmatrix} = \frac{1}{\pi^2} \sum_{\vec{n} \in \mathbb{Z}^3} \int_0^\Lambda d^3y e^{iL\vec{n} \cdot \vec{y}} \left[\mathbf{M}_2(\vec{y}) \mathcal{Z}(\vec{p}, \vec{y}) + \mathbf{M}_3(\vec{y}) \frac{2H(\Lambda)}{\Lambda^2} \right] \begin{pmatrix} \mathcal{F}_t(\vec{y}) \\ \mathcal{F}_s(\vec{y}) \end{pmatrix} \quad (5)$$

where $\mathcal{Z}(\vec{p}, \vec{y}) = [p^2 + \vec{p} \cdot \vec{y} + y^2 - E_3]^{-1}$. The matrix-valued functions $\mathbf{M}_2(\vec{y})$ and $\mathbf{M}_3(\vec{y})$ are given by

$$\mathbf{M}_2(\vec{y}) = \begin{pmatrix} -d_t(\vec{y}) & 3d_s(\vec{y}) \\ 3d_t(\vec{y}) & -d_s(\vec{y}) \end{pmatrix}, \quad \mathbf{M}_3(\vec{y}) = \begin{pmatrix} -d_t(\vec{y}) & d_s(\vec{y}) \\ d_t(\vec{y}) & -d_s(\vec{y}) \end{pmatrix}, \quad (6)$$

where $d_{s,t}(\vec{y}) = (g_{s,t}^2/8\pi)D_{s,t}(E_3 - \vec{y}^2/2, \vec{y})$ depends only on the absolute value of \vec{y} . The integral equations (5) obey Wigner SU(4) symmetry in the ultraviolet. As a consequence, a SU(4)-symmetric three-body interaction with running coupling $H(\Lambda)$ is sufficient for renormalization [11].

In a finite cubic box, spherical symmetry is broken down to cubic symmetry. As a consequence, the infinitely many irreducible representations of the double cover of the rotational group, SU(2), become reducible in terms of the eight irreducible representations of the double cover of the cubic group, 2O . The triton has $j = 1/2$. This partial wave is contained in the G_1^+ representation, which also contains $j = 7/2, 9/2, \dots$ [32]. Assuming that the triton amplitude in finite volume transforms under the G_1^+ representation, it is possible to decompose it into the different partial waves [33, 34] as

$$\mathcal{F}(\vec{y}) = \sum_{j=\frac{1}{2}, \frac{7}{2}, \dots}^{(G_1^+)} \sum_t F^{(j,t)}(y) \sum_{m_j} \tilde{C}_{jtm_j} |jm_j\rangle. \quad (7)$$

The coefficients \tilde{C}_{jtm_j} can be determined by explicitly decomposing the reducible representations [34] and the sum over t is needed if a partial wave is contained more than once. Since this is not the case for partial waves less than $13/2$, we will omit this index in the following. The vectors $|jm_j\rangle$ are given by $|jm_j\rangle = \sum_{m,s} C_{\ell(j)m\frac{1}{2}s}^{jm_j} |\ell(j)m\rangle \otimes |\frac{1}{2}s\rangle$, where the C 's are Clebsch-Gordan coefficients, $|\ell m\rangle$ is a spherical harmonic and $|\frac{1}{2}s\rangle$ is a spin-1/2 spinor. The sign in $\ell(j) = j \pm \frac{1}{2}$ has to be chosen such that $\ell(j)$ is even in order to get the positive parity of the triton.

Projecting out the J th partial wave and performing the angular integrations in Eq. (5) yields an infinite set of coupled equations:

$$\begin{aligned} \begin{pmatrix} F_t^{(j)}(y) \\ F_s^{(j)}(y) \end{pmatrix} &= \frac{4}{\pi} \int_0^\Lambda \frac{dy y^2}{2\ell(J) + 1} \sum_j^{(G_1^+)} \left[\mathbf{M}_2(y) Z^{(\ell(J))}(p, y) + \mathbf{M}_3(y) \frac{2H(\Lambda)}{\Lambda^2} \delta_{\ell(J),0} \right] \begin{pmatrix} F_t^{(j)}(y) \\ F_s^{(j)}(y) \end{pmatrix} \\ &\times \left[\delta_{Jj} + \sum_{\substack{\vec{n} \in \mathbb{Z}^3 \\ \vec{n} \neq \vec{0}}} \sqrt{4\pi} \sum_{\ell'} i^{\ell'} j_{\ell'}(L|\vec{n}|y) \sqrt{\frac{(2\ell(j) + 1)(2\ell' + 1)}{2\ell(J) + 1}} \right. \\ &\times \left. \sum_{m(\ell(j)), s(\frac{1}{2})} \frac{\tilde{C}_{j,m+s}}{\tilde{C}_{JM}} Y_{\ell(M-s-m)}^*(\hat{n}) C_{\ell(J)(M-s)\frac{1}{2}s}^{JM} C_{\ell(j)m\frac{1}{2}s}^{j,m+s} C_{\ell(j)0\ell'0}^{\ell(J)0} C_{\ell(j)m\ell'(M-s-m)}^{\ell(J)(M-s)} \right]. \end{aligned} \quad (8)$$

The notation $m(\ell)$ is used to indicate summation over $m = -\ell, \dots, \ell$. The partial waves of \mathcal{Z} are given by

$$Z^{(\ell)}(p, y) = \frac{2\ell + 1}{py} Q_\ell \left(\frac{p^2 + y^2 - E_3}{py} \right), \quad (9)$$

where Q_ℓ is a Legendre function of the second kind. Note that the δ_{Jj} -term in Eq. (8)

reproduces the infinite volume result. This equation is now specialized to the case $J = 1/2$:

$$\begin{aligned} \begin{pmatrix} F_t^{(\frac{1}{2})}(y) \\ F_s^{(\frac{1}{2})}(y) \end{pmatrix} &= \frac{4}{\pi} \int_0^\Lambda dy y^2 \sum_j^{(G_1^+)} \left[\mathbf{M}_2(y) Z^{(0)}(p, y) + \mathbf{M}_3(y) \frac{2H(\Lambda)}{\Lambda^2} \right] \begin{pmatrix} F_t^{(j)}(y) \\ F_s^{(j)}(y) \end{pmatrix} \\ &\times \left[\delta_{j\frac{1}{2}} + \sum_{\substack{\vec{n} \in \mathbb{Z}^3 \\ \vec{n} \neq \vec{0}}} \sqrt{4\pi} i^{\ell(j)} j_{\ell(j)}(L|\vec{n}|y) \sum_{m(\ell(j))} (-1)^m \tilde{C}_{j,m+M} C_{\ell(j)m\frac{1}{2}M}^{j_{m+M}} Y_{\ell(j)m}(\hat{n}) \right]. \end{aligned} \quad (10)$$

Since the leading term in the expansion of the Bessel functions in Eq. (10) is $1/(L|\vec{n}|y)$, these contributions are suppressed by at least a/L . They will be small for volumes not too small compared to the size of the bound state. The lowest partial wave that is mixed with $J = 1/2$ is the $J = 7/2$ wave. Contributions from higher partial waves will be suppressed kinematically for shallow states with small binding momentum. This is ensured by the spherical harmonic in the second term of Eq. (10). Only for small lattices, i.e. when a/L is large, this behavior is counteracted by terms stemming from the spherical Bessel function $j_{\ell(j)}(L|\vec{n}|y)$ and higher partial waves may contribute significantly. In this first study, we will therefore neglect contributions from higher partial waves. We are encouraged to do so by our results for the bosonic case, where calculations including one more partial wave yielded corrections on the percent level even for small volumes [19]. Thus, only two coupled integral equations remain. Details of the numerical methods used to solve these equations can also be found in [19].

In the following, we will present our results for the energy of the triton for cubic volumes with various edge lengths L . In order to verify that the results are properly renormalized, we produced two data sets. For one set, the cutoff was set to $\Lambda = 600$ MeV and the three-body coupling was chosen such that the triton binding energy is reproduced in the infinite volume. For the other set, the cutoff was chosen such that the three-body force vanishes for the physical triton binding energy in the infinite volume. This is always possible due to the limit cycle behavior of the three-body force. Both data sets should agree if the renormalization has been carried out properly.

Figure 2 shows the triton binding energy for finite cubic volumes with edge lengths L ranging from 17 fm down to 2 fm. The values from our two data sets (squares and circles) are in good agreement, indicating that our results are indeed cutoff independent. For large volumes, the deviation of the triton energy from its infinite volume value is small. When going to edge lengths smaller than about 10 fm, the energy of the state strongly decreases. Near $L = 6$ fm, the shift is already more than 100%. The dependence of the energy on L can be nicely fitted to a function of the form

$$E_3(L) = E_3(L = \infty) \left[1 + \frac{c}{L} e^{-L/L_0} \right], \quad (11)$$

indicated by the solid line in Fig. 2. We find the values $L_0 = 2.9$ fm and $c = 39$ fm. The length scale L_0 is associated with the size of the physical triton wave function. Thus the L -dependence of the triton energy is similar to the behavior in the two-body sector [35, 36].

The triangles give the results from a lattice calculation using chiral EFT at N²LO by Epelbaum and collaborators [20]. While they agree with our results for $L \gtrsim 10$ fm, the finite volume shifts are larger for smaller volumes. This discrepancy could be due to the fact that Epelbaum et al. calculate the volume dependence of the lowest state in the G_1^+

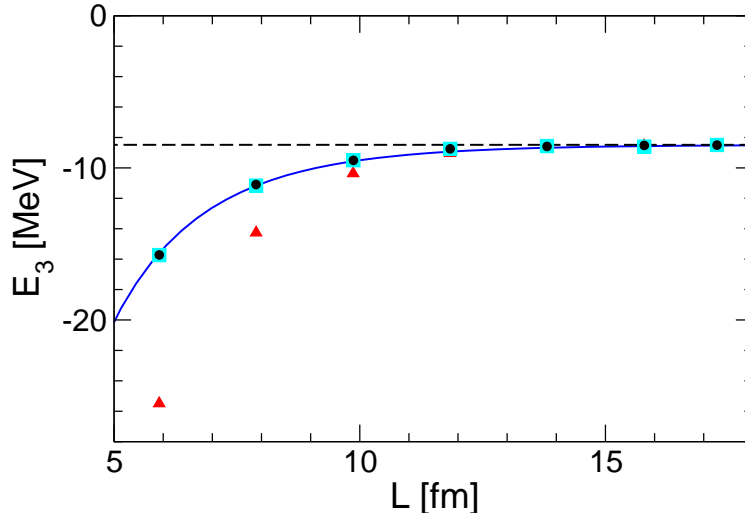


FIG. 2: Triton energy E_3 for different edge lengths L of the cubic volume. Squares and circles are data sets for different cutoffs. The triangles are from a nuclear lattice calculation using chiral EFT at N²LO [20]. The horizontal dashed line indicates the physical triton binding energy, while the solid line is a fit to our results (see text).

representation, while we focus only on the $j = 1/2$ contribution. For small volumes, the contribution of higher partial waves is expected to be more important. The inclusion of higher partial waves in our approach is in principle straightforward but numerically expensive. In our previous work for spinless bosons [19], we found the contribution of higher partial waves to be of the order a few percent for L about three times the size of the calculated state. The contribution of higher partial waves in the triton will be studied in detail in a future publication.

The next-to-leading order corrections to our results are given by the effective ranges in the 1S_0 and 3S_1 channels. There are corrections of order r_e/a and corrections of order kr_e where r_e is the effective range and k is a typical momentum. The corrections of the first type are of order 30%. They are dominated by the spin-triplet channel where the scattering length is about a factor three larger than the effective range. The corrections of the second type can be estimated from the typical momentum in the triton. Assuming that the binding momentum is shared between the nucleons in the triton, these corrections are of order 40% for large volumes and grow as L is decreased. Higher orders in the pionless EFT are required for more precise extrapolations.

In the following, we present results for the triton and its excited states near the critical pion mass $M_\pi^{crit} \approx 197$ MeV. The pion-mass dependence of the input quantities is obtained from a chiral EFT calculation [30]. These input quantities are now used to determine the coupling constants of the “pionless” EFT, as has been described for the infinite volume case in [31]. As already stated above, no additional input is needed to produce renormalized finite volume results. The pion mass dependence of the triton ground state E_3 is shown in Fig. 3 for volumes with edge lengths $L = 4.925$ fm, 3.94 fm, and 2.955 fm by the upper, middle, and lower dashed lines, respectively. The infinite volume limit is given by the solid line. Again, we plot two data sets obtained using two different cutoffs as described above which agree well with each other. The most pronounced effect of the finite volume is a strong downward shift, as was expected from the results for the triton at the physical point.

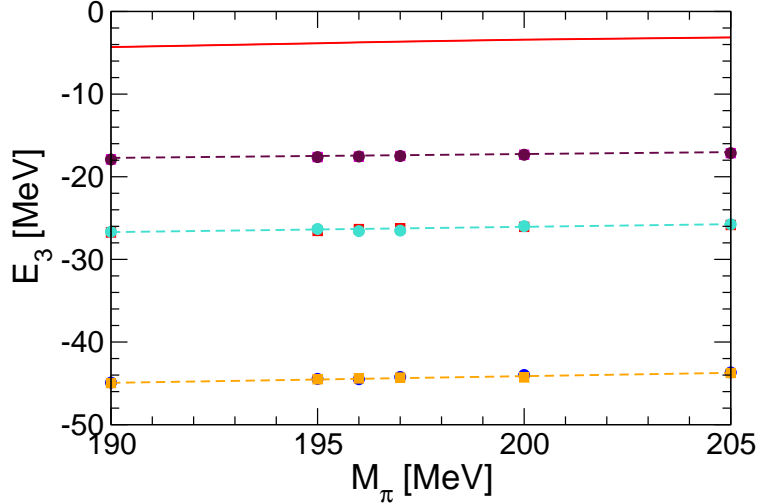


FIG. 3: Pion-mass dependence of the triton energy E_3 in the vicinity of the critical pion mass $M_\pi^{crit} \approx 197$ MeV. The solid line gives the infinite volume limit, while the upper, middle, and lower dashed line corresponds to edge lengths $L = 4.925$ fm, 3.94 fm, and 2.955 fm, respectively.

Moreover, the slope of the pion-mass dependence of E_3 depends on the size of the box L . From a linear fit to the pion-mass dependence of the triton energy in finite and infinite volume near the critical pion mass, we obtain the slopes $\Delta E_3/\Delta M_\pi = 0.0783, 0.0467, 0.064,$ and 0.08 for the edge lengths $L = \infty, 4.925$ fm, 3.94 fm, and 2.955 fm, respectively. As the volume is decreased, the slope decreases and is smallest around $L = 5$ fm. When L is decreased even further the slope increases again.

The behavior of the first excited state when put inside a finite volume is different. For large volumes, the state remains again unaffected at first. When going to smaller volumes, the energy starts to decrease strongly. But eventually the “breakup threshold”, i.e. the energy of the relevant two-body bound state in finite volume, becomes equal to the three-body energy. For pion masses smaller than M_π^{crit} , the relevant two-body bound state corresponds to the deuteron, while for $M_\pi > M_\pi^{crit}$, there is a “spin-singlet deuteron” in the 1S_0 channel and the deuteron has become a virtual state. For even smaller volumes, no triton excited state can be found. This behavior is shown in Fig. 4. The dashed lines give the energies of the deuteron ($M_\pi < M_\pi^{crit}$) and spin-singlet deuteron ($M_\pi > M_\pi^{crit}$) calculated according to [35]. The circles, squares, and triangles give the energies of the triton ground state, first excited state, and second excited state, respectively. Presumably, the triton excited state has crossed into the scattering regime where it would be driven away from threshold. We previously observed such a behavior in our investigation of three-boson bound states inside finite volumes [19]. Whether there is a universal relation between the binding energy in infinite volume and the volume size, at which the state disappears, is an interesting question that will be investigated in the future. The very weakly bound second excited state, that appears in the infinite volume for pion masses close to the critical one, could not be observed for the volumes with edge lengths of several fm that we investigated and, by the above reasoning, has crossed the threshold already at some much larger volume. This behavior of the excited states makes it difficult to study the conjectured limit cycle in Lattice QCD calculations since very large volumes are required to observe the excited states.

In this letter, we have studied the triton inside a finite cubic volume of edge length L with

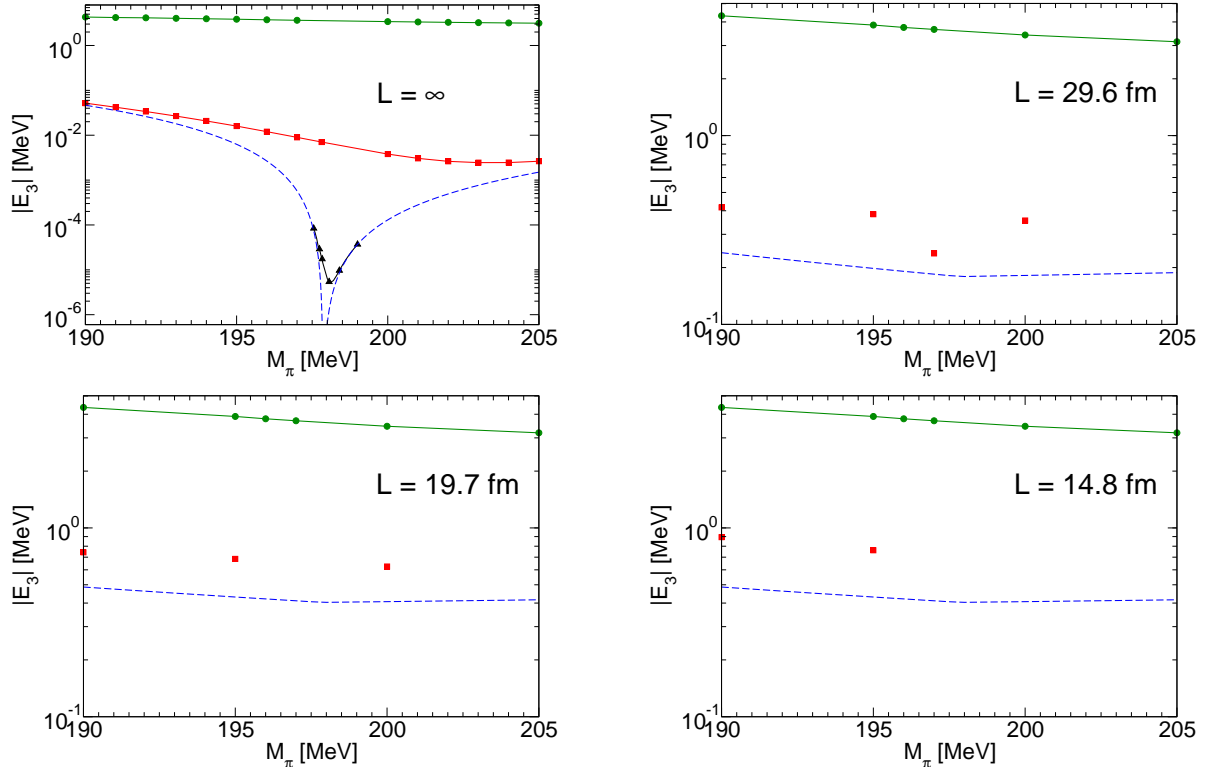


FIG. 4: Pion-mass dependence of the triton spectrum near the critical pion mass for the infinite volume and boxes with edge lengths $L = 29.6, 19.7, 14.8$ fm (from left to right and top to bottom). The dashed lines are the energies of the deuteron ($M_\pi < M_\pi^{crit}$) and spin-singlet deuteron ($M_\pi > M_\pi^{crit}$). The circles, squares, and triangles give the energies of the triton ground state, first excited state, and second excited state, respectively.

periodic boundary conditions. The knowledge of the modifications of the triton energy by a finite volume is crucial to the understanding of lattice simulations in this channel. Using the framework of the pionless EFT at leading order, we have derived an infinite set of coupled integral equations for the partial waves of the two relevant amplitudes. This equation was solved for several finite volumes of an order of magnitude typical for present day Lattice QCD calculations. Proper renormalization of the solutions was verified explicitly. We have investigated the physical triton as well as the triton and its excited states near the critical pion mass M_π^{crit} , where the two-body scattering lengths in both channels could be tuned to diverge simultaneously [22]. We found that with present day volumes, the predicted excited states of the triton cannot be observed as bound states.

The next step in our study is the inclusion of higher partial waves, which is straightforward but numerically tedious. From our previous work for spinless bosons [19], we expect the contribution of higher partial waves to be a few percent for $L \gtrsim 3a$. Corrections from higher orders of the pionless EFT should be included for practical applications of the volume dependence in extrapolations. Work in these directions is in progress. So far, our calculations have been carried out for negative energies. While our theory is completely general, the numerical treatment of positive energies above the deuteron breakup threshold requires further work. Finally, an estimate of finite temperature effects would also be useful as lattice simulations are always performed at a small, non-zero temperature.

We note that an extension of the Lüscher formula relating the infinite volume scattering phase shifts to the discrete energy levels in a finite volume [9] is implicitly contained in our work. It provides the framework to determine the low-energy constants of the pionless EFT in the two- and three-body sector from discrete energy levels in a cubic box. After this has been done, the infinite volume scattering observables can be calculated in the pionless EFT. An alternative is given by using a harmonic confinement instead of a cubic box. Luu and collaborators have shown how to reconstruct the two-body scattering phase shifts from the discrete energy levels in harmonic confinement [37]. This method might be useful for calculations of nuclear scattering amplitudes in effective approaches with nucleon degrees of freedom.

In summary, our results demonstrate that the finite volume corrections for lattice simulations of the triton are calculable and under control. With high statistics Lattice QCD simulations of three-baryon systems within reach [21], the calculation of the structure and reactions of light nuclei appears feasible in the intermediate future.

Acknowledgments

We thank Dean Lee, Ulf Meißner, Daniel Phillips, and Martin Savage for discussions. We acknowledge the hospitality of the Institute for Nuclear Theory in Seattle, where part of this work was carried out. This research was supported by the DFG through SFB/TR 16 “Subnuclear structure of matter” and the BMBF under contracts No. 06BN9006.

-
- [1] S. R. Beane, K. Orginos and M. J. Savage, *Int. J. Mod. Phys. E* **17**, 1157 (2008) [arXiv:0805.4629 [hep-lat]].
 - [2] S. R. Beane, W. Detmold, K. Orginos and M. J. Savage, arXiv:1004.2935 [hep-lat].
 - [3] S. R. Beane, P. F. Bedaque, W. C. Haxton, D. R. Phillips and M. J. Savage, arXiv:nucl-th/0008064.
 - [4] P. F. Bedaque and U. van Kolck, *Ann. Rev. Nucl. Part. Sci.* **52**, 339 (2002) [arXiv:nucl-th/0203055].
 - [5] E. Epelbaum, *Prog. Part. Nucl. Phys.* **57**, 654 (2006) [arXiv:nucl-th/0509032].
 - [6] E. Epelbaum, H.-W. Hammer and U.-G. Meißner, *Rev. Mod. Phys.* **81**, 1773 (2009) [arXiv:0811.1338 [nucl-th]].
 - [7] K.G. Wilson, *Phys. Rev. D* **10**, 2445 (1974); *Nucl. Phys. Proc. Suppl.* **140**, 3 (2005) [arXiv:hep-lat/0412043].
 - [8] M. Lüscher, *Commun. Math. Phys.* **104**, 177 (1986).
 - [9] M. Lüscher, *Nucl. Phys. B* **354**, 531 (1991).
 - [10] M. Lüscher, *Nucl. Phys. B* **364**, 237 (1991).
 - [11] P. F. Bedaque, H.-W. Hammer and U. van Kolck, *Nucl. Phys. A* **676**, 357 (2000) [arXiv:nucl-th/9906032].
 - [12] B. Borasoy, H. Krebs, D. Lee and U.-G. Meißner, *Nucl. Phys. A* **768**, 179 (2006) [arXiv:nucl-th/0510047].
 - [13] V. Efimov, *Phys. Rev. C* **44**, 2303 (1991).
 - [14] H.-W. Hammer and T. Mehen, *Nucl. Phys. A* **690**, 535 (2001) [arXiv:nucl-th/0011024].

- [15] P. F. Bedaque, G. Rupak, H. W. Griesshammer, and H.-W. Hammer, Nucl. Phys. A **714**, 589 (2003) [arXiv:nucl-th/0207034].
- [16] H. W. Griesshammer, Nucl. Phys. A **744**, 192 (2004) [arXiv:nucl-th/0404073].
- [17] L. Platter, Phys. Rev. C **74**, 037001 (2006) [arXiv:nucl-th/0606006].
- [18] S. Kreuzer and H.-W. Hammer, Phys. Lett. B **673**, 260 (2009) [arXiv:0811.0159 [nucl-th]].
- [19] S. Kreuzer and H.-W. Hammer, Eur. Phys. J. A **43**, 229 (2010) [arXiv:0910.2191 [nucl-th]].
- [20] E. Epelbaum, H. Krebs, D. Lee and U.-G. Meißner, Eur. Phys. J. A **41**, 125 (2009) [arXiv:0903.1666 [nucl-th]].
- [21] S. R. Beane *et al.*, Phys. Rev. D **80**, 074501 (2009) [arXiv:0905.0466 [hep-lat]].
- [22] E. Braaten and H.-W. Hammer, Phys. Rev. Lett. **91**, 102002 (2003) [arXiv:nucl-th/0303038].
- [23] S.R. Beane, P.F. Bedaque, M.J. Savage, and U. van Kolck, Nucl. Phys. A **700**, 377 (2002) [arXiv:nucl-th/0104030].
- [24] S.R. Beane and M.J. Savage, Nucl. Phys. A **717**, 91 (2003) [arXiv:nucl-th/0208021]; Nucl. Phys. A **713**, 148 (2003) [arXiv:nucl-th/0206113].
- [25] E. Epelbaum, U.-G. Meißner, and W. Glöckle, Nucl. Phys. A **714**, 535 (2003) [arXiv:nucl-th/0207089].
- [26] V. Efimov, Phys. Lett. **33B**, 563 (1970).
- [27] F. Ferlino and R. Grimm, Physics **3**, 9 (2010).
- [28] E. Braaten and H.-W. Hammer, Phys. Rept. **428**, 259 (2006) [arXiv:cond-mat/0410417].
- [29] H.-W. Hammer and L. Platter, to appear in Ann. Rev. Nucl. Part. Sci. (2010), arXiv:1001.1981 [nucl-th].
- [30] E. Epelbaum, H.-W. Hammer, U.-G. Meißner and A. Nogga, Eur. Phys. J. C **48**, 169 (2006) [arXiv:hep-ph/0602225].
- [31] H.-W. Hammer, D.R. Phillips and L. Platter, Eur. Phys. J. A **32**, 335 (2007) [arXiv:0704.3726 [nucl-th]].
- [32] R. C. Johnson, Phys. Lett. B **114**, 147 (1982).
- [33] F. C. von der Lage and H. A. Bethe, Phys. Rev. **71**, 612 (1947).
- [34] V. Bernard, M. Lage, U.-G. Meißner and A. Rusetsky, JHEP **0808**, 024 (2008) [arXiv:0806.4495 [hep-lat]].
- [35] S. R. Beane, P. F. Bedaque, A. Parreno and M. J. Savage, Phys. Lett. B **585**, 106 (2004) [arXiv:hep-lat/0312004].
- [36] D. Lee, private communication (2010).
- [37] T. Luu, M. Savage, A. Schwenk and J. P. Vary, arXiv:1006.0427 [nucl-th].